Final Report

Evaluating Sudden Stratospheric Warmings and NAM Predictability in the NMME Phase-2 System

1. General Information

Title: Evaluating Sudden Stratospheric Warmings and NAM Predictability in the NMME Phase-2 System

PI/co-PI names and institutions

- **Lead PI:** Jason C. Furtado, School of Meteorology, University of Oklahoma
- **Co-PIs:** Judah Cohen, Atmospheric and Environmental Research • Emily Becker, NOAA Climate Prediction Center • Dan Collins, NOAA Climate Prediction Center

Grant #: NA15OAR4310077

2. Main goals of the project, as outlined in the funded proposal

Quantify stratosphere-troposphere coupling processes and NAM predictability within the NMME Phase-2 system in order to identify model biases and subsequently improve sub-seasonal winter forecasts.

3. Results and accomplishments

Introduction

This project explored the predictability of sudden stratospheric warmings (SSWs) and tropospheric winter weather patterns congruent with the Northern Annular Mode (NAM) using hindcasts from the North American Multi-Model Ensemble (NMME) Project Phase-2. The results presented below are a summary of this work, which is mainly focused on model evaluation of key characteristics of the tropospheric and stratospheric NAM, lifecycle characteristics of SSWs, and both antecedent and post-SSW tropospheric weather regimes as represented in the models. Comparisons for the simulated fields were made against the ERA-Interim reanalysis and NCEP-NCAR reanalysis products (only comparisons with ERA-Interim are presented in this report). Unless otherwise noted, results from the NMME Phase-2 models are presented as ensemble-mean statistics (ten members per model) of runs with November – March initialization dates from 1982-2013.

The culmination of our work satisfies the majority of our proposed work (***Tasks #1 and #2***). However, the original proposed plan involved a comprehensive SSW predictability study (including case studies) amongst all eight (8) NMME Phase-2 models. When the proposal was written, NMME Phase-2 model developers committed to production of several daily-mean output fields, particularly at stratospheric levels, which were never produced for all models[1]. After two years of teleconferencing and working with the data masters, we were only able to analyze three (3) models with the necessary output: *CanCM3*, *CanCM4*, and *CCSM4*[2]. There is currently no effort to make more output available, hindering any further analyses. Nevertheless, our evaluations of the tropospheric and stratospheric NAM and SSWs will prove valuable for future use of these specific models if/when used in operational settings.

Representation of Tropospheric NAM Variability in the NMME Phase-2 Models

Our results begin with findings for ***Task #1*** of our proposal: quantifying key characteristics of how the models simulate the spatiotemporal characteristics of the stratospheric and tropospheric NAM. The NAM is the leading mode (i.e., leading empirical orthogonal function (EOF) / principal component (PC)) of the Northern Hemisphere (NH) extratropical geopotential height field [e.g., *Thompson and Wallace*, 1998, 2000]. As such, the tropospheric NAM physically represents changes in the strength and position of the polar jet stream and consequently storm tracks and temperature patterns. For the models, the NAM index at a given pressure level is not computed through EOF analysis directly on the model fields. Instead, daily-mean geopotential height (GPH) anomalies (GPHa) from the hindcasts are *projected onto* the characteristic

[1] The original NMME Phase-2 data plan is here: http://www.cpc.ncep.noaa.gov/products/ctb/nmme/NMME-PhaseII-DataPlan-27May.pdf. This was the plan we worked with when originally writing our proposal for this grant.

[2] The research team never received a complete hindcast dataset for the CCSM4 model but forged ahead with what we had.

NAM field at that pressure level from *reanalysis* to form the NAM time series for the model. Taking this approach allows us to avoid model biases in EOF orderings and instead focus on examining the physicality of the mode and its characteristics.

Figure 1 displays the regression of sea level pressure (SLP) anomalies (SLPa) onto the leading PC time series of 1000 hPa GPHa (i.e., the NAM_{1000} index) for reanalysis and models. At first glance, the models seem to capture well the structure of the near-surface NAM – indeed, the spatial correlations between the reanalysis and the model SLPa fields in **Fig. 1** are 0.7 – 0.9. However, there are some key differences that factor into the remainder of our evaluation. First, the Pacific nodal center of the NAM is significantly stronger in the models than in the observations. In particular, for the CanCM4 and CCSM4 ensemble-mean, the maximum SLPa associated with the NAM_{1000} exists in the Pacific, not the Atlantic as seen in observations (**Fig. 1**). Secondly, the models are slightly biased toward an east-based North Atlantic Oscillation (NAO) signature, which has an impact on the teleconnection's impact on European weather regimes in the models vs. observations.

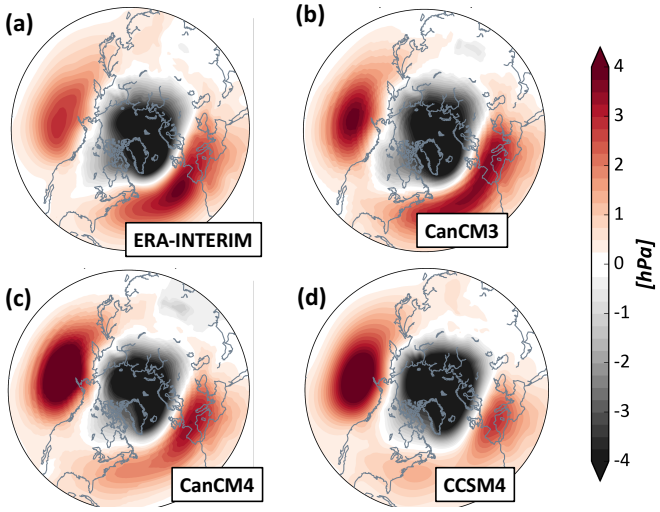

FIG. 1. (a) Regression of the November – March (NDJFM) SLPa (hPa) onto the NAM_{1000} index in ERA-Interim. (b) – (d) Same as (a) but for the ensemble-mean regressions for (b) CanCM3, (c) CanCM4, and (d) CCSM4. Regressions presented as the positive phase of the NAM_{1000}.

When examining the temporal statistics of the near-surface NAM, we find that the models *underestimate* the longevity of this internal mode of variability, particularly for negative NAM regimes. The autocorrelation functions of the NAM_{1000} index (**Figure 2**) illustrate that the Canadian models have a similar decorrelation timescale to the observed NAM_{1000} index (~12-13 days), but the CCSM4 is shorter by a couple of days. Furthermore, beyond Day 15, the autocorrelation curve of the observed NAM_{1000} index flattens considerably, while autocorrelation functions from the models continue their exponential drop. This "bump" in the observed autocorrelation likely reflects the extended persistence of negative NAM regimes. ***This feature is important both dynamically and for forecasting*****,** as jet dynamics indicate that the negative NAM regime is easier to maintain in the extratropical atmosphere [e.g., *Barnes and Hartmann*, 2010] and thus can lead to extended periods of extreme winter weather [e.g., *Thompson and Wallace*, 2001; *L'Heureux et al.*, 2009].

To test this hypothesis explicitly in the NMME Phase-2 models, we calculate the average frequency and duration of both positive and negative NAM_{1000} regimes. That is, we count the number of consecutive days that the November – March (NDJFM) NAM_{1000} index was above 1σ (+NAM) and below -1σ (–NAM) and the frequency of these occurrences. The results affirm our original hypothesis – i.e., the models have *similar* frequency spectra for both +NAM and –NAM regimes (**Figure 3**), while the observed frequency spectrum for –NAM regimes (**Fig. 3, right**, dashed black line) shows a "bump" in the frequency of persistent –NAM regimes beyond 10-15 days. ***The deficiency of the models in simulating the asymmetry of positive and negative tropospheric NAM regime durations has significant consequences when using the NMME-2 models for subseasonal winter forecasts, particularly for extreme winter weather*****.** The lack of this feature is likely because of two deficient components in the models: (1) Poor

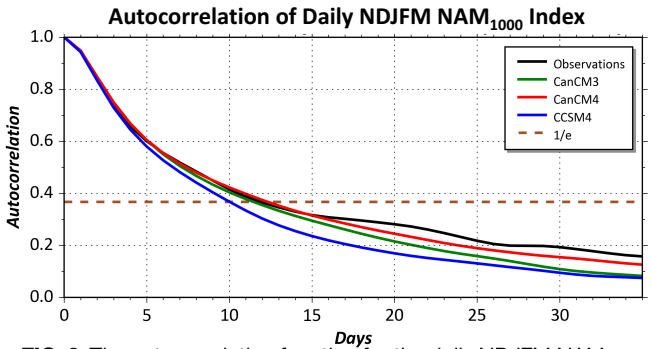

FIG. 2. The autocorrelation function for the daily NDJFM NAM_{1000} index from ERA-Interim (black), CanCM3 (green), CanCM4 (red), and CCSM4 (blue). Dashed brown line denotes $r = 1/e$.

storm track variability (indeed, the variability of North Atlantic storm tracks / polar jet is quite muted in the models compared with reanalysis – **Figure 4**); and (2) stratosphere-troposphere coupling, an important source of tropospheric NAM variability.

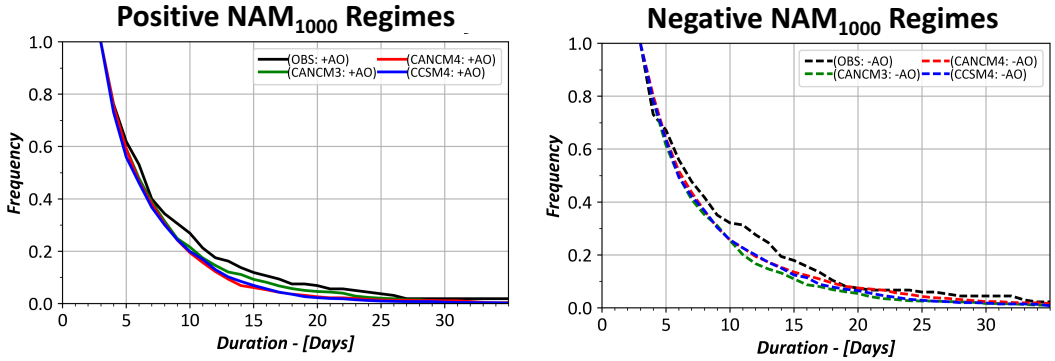

FIG. 3. (left) The frequency of positive NAM_{1000} regimes with a duration of *at least x* days (3 days minimum) in ERA-Interim (black), CanCM3 (green), CanCM4 (red), and CCSM4 (blue). (right) As in (left) but for negative NAM_{1000} regimes.

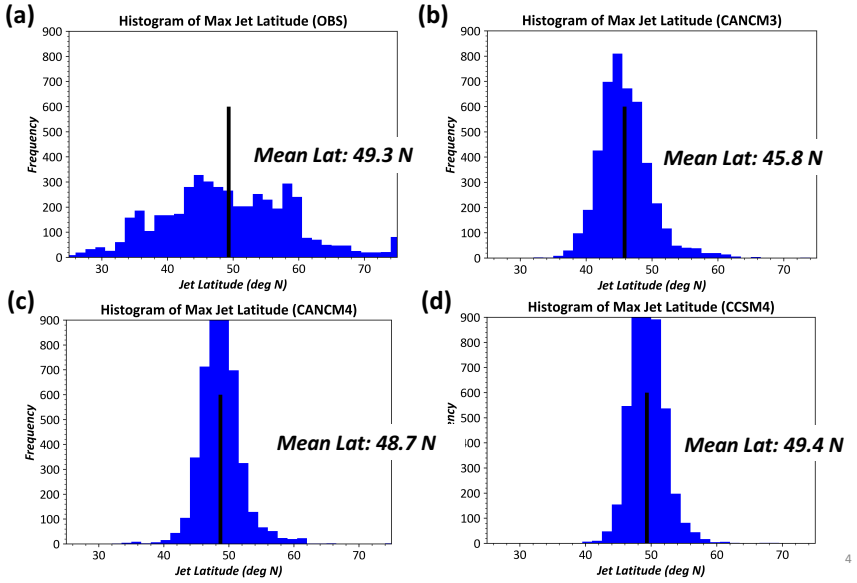

FIG. 4. (a) Histogram of the latitude where the daily maximum 850-500 hPa averaged zonal wind speed is found in the North Atlantic. Values shown from November – March. (b) – (d) As in (a) but for the ensemble-mean for (b) CanCM3, (c) CanCM4, and (d) CCSM4. Black vertical line denotes the mean latitude in the distribution. Numerical value for the mean latitude also provided. The models display narrow distributions from the models vs. the observations, indicating that the models have very low variability in the North Atlantic polar jet stream / storm tracks. This metric is also a measure of the strength and variability of the tropospheric NAM.

Representation of Stratospheric NAM Variability in the NMME Phase-2 Models

Having examined the characteristics of the tropospheric NAM in reanalysis and models, we next evaluate stratospheric NAM variability and thus fulfill ***Task #1*** of the proposed research. Note that in the stratosphere, the NAM physically represents modulation of the strength of the stratospheric polar vortex [e.g., *Thompson and Wallace*, 2000; *Baldwin and Dunkerton*, 2001]. **Figure 5** shows the regression of 50 hPa GPHa onto the NAM_{1000} index. The observed regression pattern (**Fig. 5a**) shows low heights located over the pole (i.e., the stratospheric polar vortex) encircled by higher heights in the middle latitudes. The three models generally capture this annular structure, though the CCSM4 has almost a monopole structure (i.e., "non-annular"). Nevertheless, spatial correlations between model and reanalysis fields in **Fig. 5** are high (~0.8-0.9), and thus agreement in the structure of the stratospheric polar vortex is high.

Bigger differences emerge for the variability in the strength of the stratospheric polar vortex

(**Figure 6**). Indeed, the climatological variance of the December – February (DJF) stratospheric polar vortex in all models is nearly a quarter or more less than ERA-Interim. This significant reduction in variability physically represents less-frequent disruptions of the polar vortex in the NMME Phase-2 models – i.e., less SSW events. This finding further supports the hypothesis that the models' simulated stratospheres will feature less dynamical coupling with the troposphere and therefore are less likely to have a demonstrable influence on surface weather conditions. Lower polar vortex variability in the models is a common feature in coupled climate models, as noted in previous work by the PI and others [e.g., *Charlton et al.*, 2013; *Furtado et al.*, 2015].

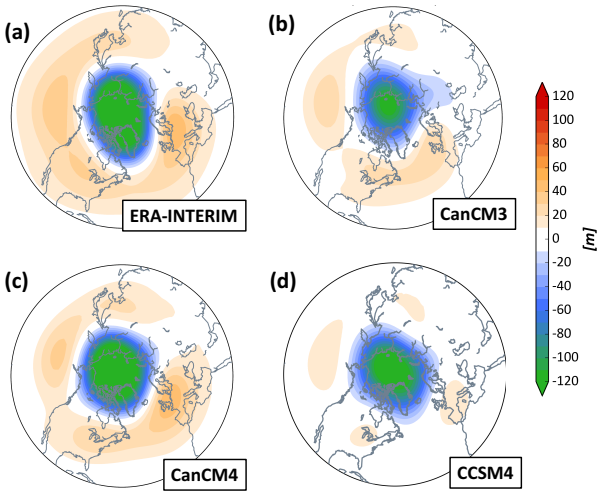

FIG. 5. As in **Fig. 1** except for NDJFM 50 hPa GPHa (m). Sign convention is for the positive phase of the stratospheric NAM.

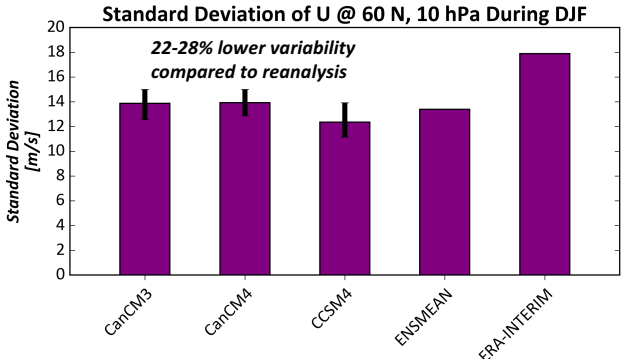

FIG. 6. The standard deviation of the zonal-mean zonal wind ([U]; m/s) at 60°N, 10 hPa from the models, the ensemble-mean of all models, and ERA-Interim. Black error bars indicate the absolute maximum and minimum of the standard deviation amongst individual ensemble members of a particular model.

Precursors and Post-SSW Impacts in *Simulated* Major SSW Events

Quantifying and evaluating the antecedent and subsequent atmospheric circulation patterns associated with major SSW events is a major tenet of our proposed work (i.e., ***Task #2***). Major_SSW events are identified in observations and the models as in *Charlton and Polvani* [2007] and *Butler and Polvani* [2011] – i.e., the central date of the major SSW is the first day where the zonal-mean zonal wind ([U]) at 60°N, 10 hPa goes easterly. Under this criterion, there are twenty (20) major SSW events between 1982 – 2013 in ERA-Interim [see also *Butler et al.*, 2015]. For the NMME Phase-2 models, because we are seeking a representative sample of *simulated* major SSWs, additional criteria are added. First, we select hindcasts with start dates in November only (i.e., the start of the extended cold season and also the start of active stratosphere-troposphere coupling season). However, because there are 320 total runs per model (10 ensemble members x 32 years), many more SSW events will be identified than in observations. Hence, for computing statistics from the models, we randomly choose ten (10) major SSWs per ensemble member per model, yielding ~100 major SSWs per model. The CCSM4 model is the exception – it has a three times *less* major SSWs overall compared to the other two models. Hence, for the CCSM4, we retain all identified major SSWs for statistical calculations. Analyses were repeated with varied sample sizes from the models (i.e., choosing only 5-10 SSW events per ensemble member). Our findings are robust to these sampling variations, strengthening our evaluation and conclusions on model performance.

Figure 7 presents the composite of 500 hPa GPHa averaged 30 to 15 days *before* a major SSW event in ERA-Interim (**Fig. 7a**) and in the NMME Phase-2 models (**Figs. 7b-7d**). This composite represents the favorable mid-tropospheric pattern to excite vertically propagating Rossby waves that eventually break

in the polar stratosphere and disrupt the polar vortex. The observed precursor pattern (**Fig. 7a**) shows two prominent centers of action that constructively interfere with the climatological standing wave pattern in the NH: (1) Anomalous ridging across northern Eurasia; and (2) an amplified North Pacific trough / subtropical North Pacific ridge pattern (i.e., the North Pacific Oscillation; NPO). These features match well with the precursor patterns shown in, e.g., *Kolstad and Charlton-Perez* [2011] and *Cohen and Jones* [2012]. Both the CanCM3 and CanCM4 recover the Eurasian ridge and the negative North Pacific height anomalies (though the CanCM4 does not recover the NPO; **Figs. 7b and 7c**). The CCSM4, however, presents a composite pattern almost *opposite* of that in reanalysis, questioning the fidelity of the CCSM4 in replicating the fundamental mechanisms associated with major SSWs and their impacts.

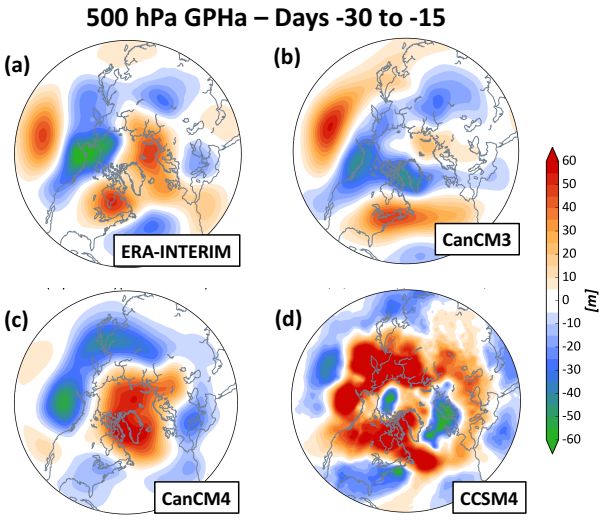

FIG. 7. (a) The composite of 500 hPa GPHa (m) from ERA-Interim averaged 30 to 15 days before the start of a major SSW (see text). (b) As in (a) but for the ensemble-mean composite from CanCM3. (c) As in (b) but for CanCM4. (d) As in (b) but for CCSM4.

To examine how the models simulate actual vertical wave propagation and its role in major SSWs, **Figure 8** examines the lag composite of the vertical component of the Eliassen-Palm flux (EPz; proportional to meridional heat flux), area-averaged from 40-80°N. In reanalysis, the largest 'pulse' or strongest poleward heat flux occurs about 5 days preceding a major SSW event (**Fig. 8**, black line). However, vertical wave propagation is actually enhanced up to 18 days before the event (i.e., "preconditioning" pulses) in reanalysis, offering a source of predictability for major SSW events on subseasonal timescales. The CanCM4 and CCSM4 replicate well the late pulse just days before a major SSW event **(Fig. 8**, red and blue lines, respectively). However, neither model simulates the preconditioning pulses in the ensemble-mean as far back as Day -18, though individual ensemble members (**Fig. 8**, gray lines) capture this, indicating significant variability in the model runs. Surprisingly, the CanCM3 shows no 'pulses' of EPz activity for all negative lags and actually suggests a *decrease* in wave activity days before the major SSW (**Fig. 8**, green line). Recall that the CanCM3 simulated correctly the antecedent 500 hPa pattern as seen in observations (**Fig. 7b**). Hence, this model clearly mishandles wave dynamics and stratosphere-troposphere coupling in general, a feature that merits further investigation.

Significant biases also exist with post-SSW impacts simulated by the NMME Phase-2 models. **Figures 9** and **10** show the composite 500 hPa GPHa (**Fig.** 9) and surface temperature anomalies (**Fig. 10**) averaged days 5 to 60 after a major SSW event. In reanalysis (**Fig. 9a**), a clear negative NAO signature exists with high (low) height anomalies featured over Baffin Bay (North Atlantic). The North Pacific basin features anomalously high pressure, signaling a weakening of the climatological Aleutian Low present after major SSW events. The CanCM3 and CanCM4 models recover the negative NAO signal, though the nodal centers are shifted further east versus reanalysis (**Figs. 9b and 9c;** see also **Fig. 1** for the noted east-based NAO bias in the models). This more east-based –NAO signature likely influences the corresponding temperature anomalies seen in the models, with much more widespread cold anomalies overspreading central and southern Europe versus what is observed (**Figure 10**). Differences in the

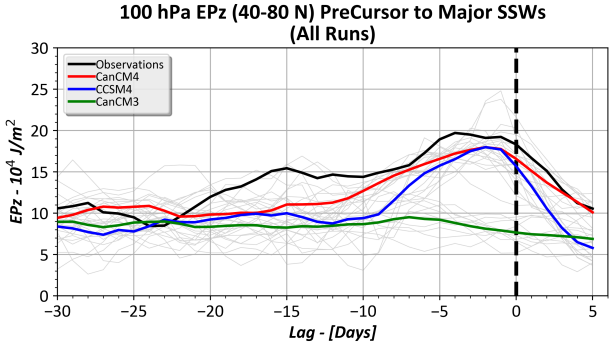

FIG. 8. Lag composite of area-averaged (40-80°N) EPz (10^4 J m^{-2}) at 100 hPa 30 days before to 5 days after a major SSW. Results shown for ERA-Interim (black) and the ensemble-mean of the CanCM3 (red), CanCM4 (green), and CCSM4 (blue). Thin gray lines represent composites from the individual ensemble members of each model. Thick dashed black line denotes day of major SSW event (i.e., Day 0).

two Canadian models emerge in the Pacific sector, however. While the CanCM3 model somewhat reproduces the positive GPHa there as in ERA-Interim (**Fig. 9b**), the CanCM4 shows the opposite – strong *negative* height anomalies in the North Pacific (**Fig. 9c**). The anomalous cyclonic circulation in the North Pacific in the CanCM4 model would consequently flood North America with milder than average temperatures (**Fig. 10c**) versus the characteristic colder conditions seen with -NAM/-NAO regimes (e.g., **Fig. 10a**). Thus, while the CanCM4 has performed well with other metrics, forecast confidence and skill for sensible weather (temperature and precipitation) patterns across North America especially is lower than expected. Finally, the CCSM4 is yet again the poorest simulator of post-SSW impacts, with a very weak –NAO signature (**Fig. 9d**) and the wrong sign of temperature anomalies for much of North America and Europe (**Fig. 10d**).

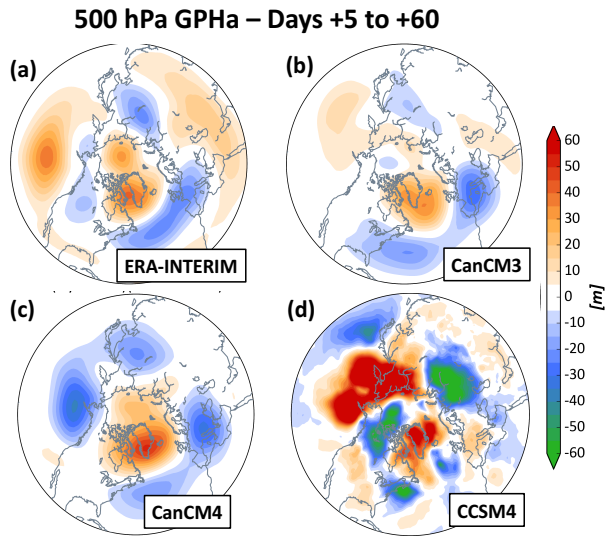

FIG. 9. As in **Fig. 7** but for the composite for days +5 to +60 following a major SSW event.

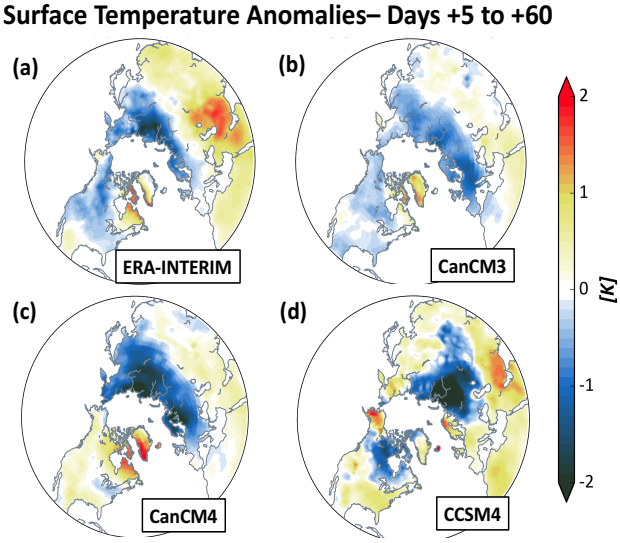

FIG. 10. As in **Fig. 9** but for surface temperature anomalies (K).

Figure 11 depicts the lag composite of the daily-mean NAM_{1000} index 0 to 60 days after a major SSW event for the ERA-Interim and the models. In reanalysis (**Fig. 11**, black line), the NAM_{1000} index takes a significant dive through Day +20 after a major SSW, recovers slightly, and then remains predominantly negative through Day +60. This extended –NAM regime signals a prolonged period of cold and potentially stormy weather for major population centers in the NH extratropics. The models, however, show a different evolution. While the models simulate an immediate negative response to the NAM_{1000} index following a major SSW (though of lower magnitude), the NAM_{1000} index recovers rather quickly and turns positive by Day +35 to +40 in the CCSM4 and CanCM3 models (**Fig. 11**, blue and green lines, respectively). Only the CanCM4 shows consistently negative NAM_{1000} index values throughout the period (**Fig. 11**, red line). This fact could explain why the CanCM4 recovers well the –NAO pattern and consequently the Eurasian cold temperature pattern following major SSW events (**Figs. 9c** and **10c**). Because North America has a variable response to strongly negative surface-based NAM conditions (i.e., the Pacific node is actually the key controller for North American winter weather temperature and precipitation patterns), the CanCM4 may not be ideal for North American winter

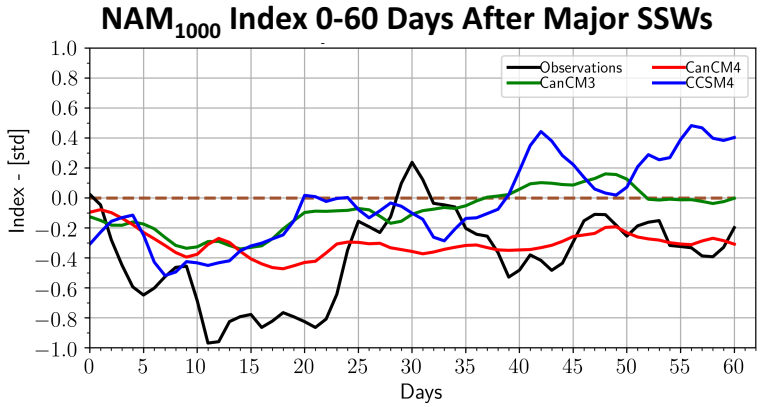

FIG. 11. Lag composite of the NAM_{1000} index 0 to 60 days following a major SSW event for ERA-Interim (black), CanCM3 (green), CanCM4 (red), and CCSM4 (blue). Dashed brown line denotes the zero value for NAM_{1000}.

weather regimes when considering post-major SSW impacts.

Examining Stratosphere-Troposphere Dynamics in the NMME Phase-2 Models

The final part of the results for ***Task #2*** involves quantification of metrics of stratosphere-troposphere dynamical coupling in the models. The first diagnostic we present is lagged composites of the NAM index as a function of pressure – i.e., a replication of the seminal 'dripping paint' plots of *Baldwin and Dunkerton* [2001] (**Figure 12**). The ERA-Interim plot (**Fig. 12a**) matches well the findings from *Baldwin and Dunkerton* [2001] – i.e., the strong negative NAM values at day 0 at 10 hPa (representing a weakened vortex) propagate downward through the stratosphere and eventually cross into the troposphere, indicating a general weakening and equatorward shift of the tropospheric polar jet stream weeks following the SSW event. **Figs. 12b – 12d** show the same NAM lag composites but for the NMME Phase-2 models. Only the CanCM4 (**Fig. 12c**) reproduces the downward propagation elements of the NAM following major SSWs. The CanCM3 (**Fig. 12b**) shows virtually no downward propagation signal associated with major SSWs. The CCSM4 model displays downward propagation of the negative NAM signal within the stratosphere but with minimal descent into the troposphere (**Fig. 12d**). The lack of the downward propagation signal in stratosphere-troposphere coupling studies involving coupled climate models is a commonly missed feature [e.g., *Furtado et al.*, 2015], particularly models with a "low-top" [e.g., *Charlton-Perez et al.*, 2013]. Hence, our findings suggest that ***stratospheric circulation anomalies are divorced from influencing, directly or remotely, tropospheric weather patterns in these NMME Phase-2 models***, ***unlike what observations and dynamics dictate should happen*****.**

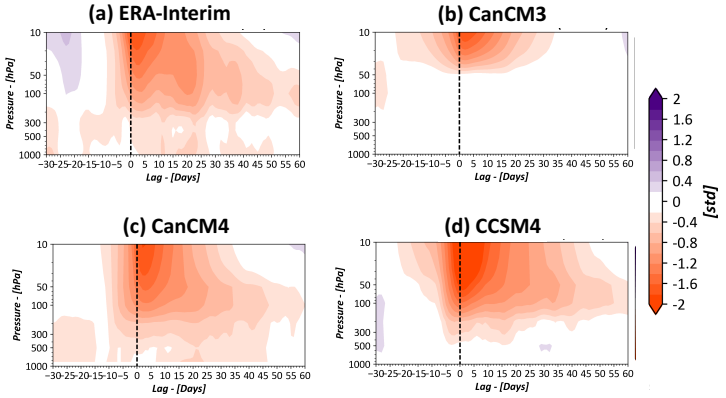

FIG. 12. (a) Lag composite of the NAM index as a function of pressure level for major SSW events in ERA-Interim. (b)-(d) As in (a) but for *simulated* major SSWs in the (b) CanCM3, (c) CanCM4, and (d) CCSM4. Negative (positive) lags indicate days before (after) a major SSW. Day 0 (i.e., the central date for the major SSW event) indicated with vertical dashed black line.

To try to understand what could be dynamically wrong with the models in their "downward propagation", we examine how wave fluxes in the troposphere respond to major SSWs in the models. In observations, prior work done by the PI and others [e.g., *Kushner and Polvani*, 2004; *Song and Robinson*, 2004; *Thompson et al.*, 2006] indicates that the tropospheric response to SSWs resembles a rearrangement or change in horizontal and vertical propagation of tropospheric waves. That is, as the vertical shear across the tropopause changes after a major SSW (through the presence of anomalous easterly winds), tropospheric baroclinic eddies move anomalously poleward, and vertical wave propagation is muted. As such, this change in horizontal wave motions works to pump westerly momentum *equatorward*, and thus shift the polar jet stream equatorward (i.e., develop negative NAM conditions; *Thompson et al.*, 2006). Therefore, in order for the models to correctly simulate the downward influence of the stratosphere onto the troposphere, they must replicate these changes in tropospheric wave fluxes**.** As **Figure 13** indicates, the models do not have this key dynamical principle, at least not as is simulated in reanalysis. Thus, the NMME Phase-2 models ***cannot be expected to recover the canonical negative NAM conditions following major SSW events***. This lack of the change in wave dynamics is consistent with the previous results shown, including the lack of a sustained $-NAM_{1000}$ signature in the models (**Fig. 11**) and the muted variance in North Atlantic storm tracks and overall meridional vacillations in the polar jet stream (**Fig. 4**).

Taken together, our findings indicate that the NMME Phase-2 models have some faithful reproductions of fundamental statistics of the polar vortex and of the near-surface NAM. However, when we explicitly explore the dynamics involved with stratosphere-troposphere coupling, models disagree and even miss key facets of this dynamical coupling. Thus, while the models may have some signatures of

negative NAM conditions in the troposphere following major SSW events (e.g., **Fig. 11**) they may be getting them for the wrong reasons. ***Our analysis identifies a key deficiency in the NMME Phase-2 models and offers caution on using these three models for extended predictability related to stratosphere-troposphere coupling***. This result may actually hold whether or not a major SSW event is involved, as our diagnosis of the spatiotemporal characteristics of the tropospheric NAM highlighted some notable biases.

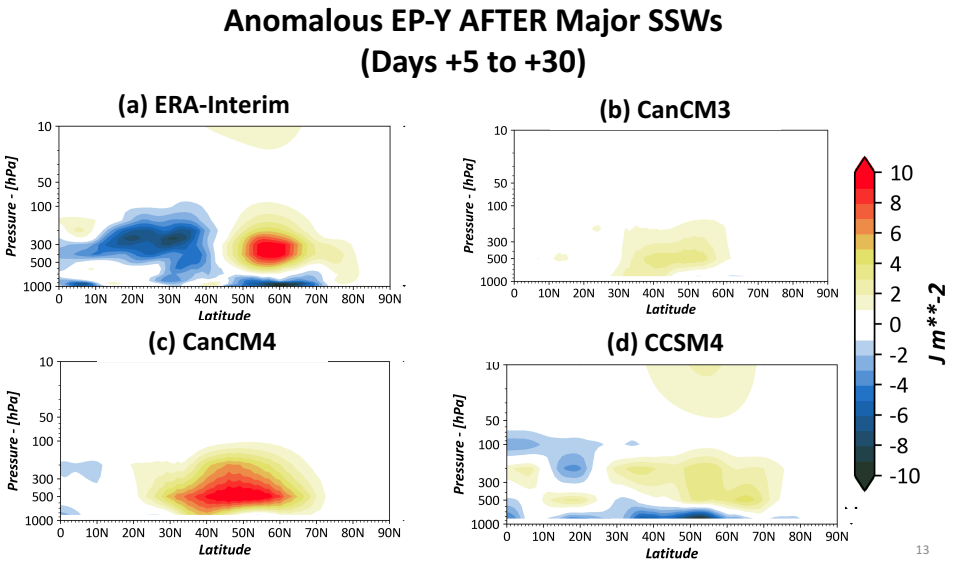

FIG. 13. (a) Composite of the *y* component of the EP flux (EPy; 10^4 J m^{-2}; proportional to *negative* momentum flux) for days +5 to +30 after a major SSW event. The strong positive-negative dipole in the upper troposphere seen near 45°N indicates the equatorward shift of the polar jet stream, characteristic of the negative NAM regime in the troposphere (e.g., **Fig. 11**). (b) As in (a) but for the CanCM3 ensemble-mean. (c) As in (a) but for the CanCM4 ensemble-mean. (d) As in (a) but for the CCSM4 ensemble-mean.

4. Highlights of Accomplishments

- Even with very limited model output available to the research team, we have accomplished ***Tasks #1 and Task #2*** of the original proposal. As such, results are limited to three models.
- The NMME Phase-2 models reproduce several spatiotemporal characteristics of the near-surface NAM. Important differences, however, emerge in the Pacific nodal center of the tropospheric NAM and with the lack of extended frequency of long-duration –NAM regimes in the analyzed NMME Phase-2 models. The models also feature far less variability in the meridional excursions of the North Atlantic polar jet stream than seen in reanalysis. These facets have strong implications on forecasts for North America and also with predictability of extreme winter weather periods prevalent during –NAM regimes.
- The NMME Phase-2 models which we analyzed reproduce well the structure of the NH stratospheric polar vortex, but the variability in the strength of the stratospheric polar vortex is nearly 25-30% less than what is observed. This lack of variability physically represents the lowered frequency of vortex breakdowns simulated by the models and hint at problems with stratosphere-troposphere coupling dynamics in the models.
- Composites of precursor conditions to major SSWs in observations shows an amplified wave-1 / wave-2 structure in the middle troposphere across Eurasia and the Pacific-North America sector. For simulated SSWs, only the Canadian models simulate this precursor mid-tropospheric pattern well. When specifically examining the vertical wave propagation in the models versus reanalysis, the CanCM4 and CCSM4 recover the major vertical wave pulse just days before a major SSW.

However, none of the models show the preconditioning vertical wave pulses occurring 10-20 days before a major SSW as suggested by reanalysis. This absence limits the models' ability to be used for subseasonal predictions of SSW events.

- Post-SSW impacts as reflect by the subsequent tropospheric circulation pattern tend to agree best in the Atlantic sector in all models. Yet, the models are divergent in their sensible weather impacts. The two Canadian models have completely opposite circulation patterns in the North Pacific, yielding different subseasonal temperature forecasts / impacts across North America. The CCSM4 is an overall poor performer in all aspects of post-SSW circulation anomalies.
- When examining downward propagation signatures of the NAM, the models demonstrate known biases in coupled climate models – i.e., a lack of downward propagation of stratospheric anomalies into the troposphere. This lack of downward propagation may be tied to the inability of the models to simulate correctly the rearrangement of the tropospheric wave propagation characteristics and the observed flux divergence in the troposphere, yielding a sustained equatorward displacement of the polar jet stream. Thus, these models should be used cautiously for extreme winter weather predictions typically associated with –NAM regimes.

5. Transitions to Applications

No formal transitions to applications have been conducted with the results of this study. Part of the reason is that we were only able to evaluate three models and at least one (CCSM4) with some missing output. However, PI Furtado delivered a presentation on these results as a webinar to NOAA MAPP participants, at the American Meteorological Society (AMS) meeting in January 2017, and also at the 42nd Annual NOAA Climate Diagnostics and Prediction Workshop in October 2017. NOAA CPC operational forecasters and research scientists attended these presentations and questioned PI Furtado on the findings.

6. Publications from the Project

Kretschmer, M., D. Coumou, L. Agel, M. Barlow, E. Tziperman, and J. Cohen, 2017: More-persistent weak stratospheric polar vortex states linked to cold extremes. *Bull. Amer. Meteor. Soc.*, doi: 10.1175/BAMS-D-16-0259.1

7. PI Contact Information

Jason C. Furtado
University of Oklahoma School of Meteorology
120 David L. Boren Blvd. Suite #5900
Norman, OK 73072
Phone: 405-325-1391
Email: jfurtado@ou.edu

References

Baldwin, M. P., and T. J. Dunkerton, 2001: Stratospheric harbinger of anomalous weather regimes,

Science, 294, 581 – 584.

Barnes, E. A., and D. L. Hartmann, 2010: Dynamical feedbacks and the persistence of the NAO. *J. Atmos. Sci.*, **67**, 851-865.

Butler, A. H. and L. M. Polvani, 2011, El Niño, La Niña, and stratospheric sudden warmings: A reevaluation in light of the observational record, *Geophys. Res. Lett.*, *38*, doi: 10.1029/2011GL048084.

Butler, A. H., D. J. Seidel, S. C. Hardiman, N. Butchart, T. Birner, and A. Match, 2015: Defining sudden stratospheric warmings. *Bull. Amer. Meteor. Soc.*, **96**, 1913 – 1928.

Charlton, A. J. and L. M. Polvani, 2007, A new look at stratospheric sudden warmings. Part I: Climatology and modeling benchmarks, *J. Climate*, *20*, 449 – 469.

Charlton-Perez, A. J., and Coauthors, 2013: On the lack of stratospheric dynamical variability in the low-top versions of the CMIP5 models. *J. Geophys. Res.*, **118**, 2494–2505.

Cohen, J. and J. Jones, 2012, Tropospheric precursors and stratospheric warmings, *J. Climate*, *25*, 1780 – 1790.

Furtado, J. C., J. L. Cohen, A. H. Butler, E. E. Riddle, and A. Kumar (2015), Eurasian snow cover variability and links to winter climate in the CMIP5 models, *Climate Dyn.*, *45*, 2591 – 2605.

Kolstad, E. W., and A. J. Charlton-Perez, 2011: Observed and simulated precursors of stratospheric polar vortex anomalies in the Northern Hemisphere. *Climate Dyn.*, *37*, 1443 – 1456.

Kushner, P.J. and L.M. Polvani, 2006: Stratosphere–troposphere coupling in a relatively simple AGCM: The role of eddies. *J. Climate,* **17**, 629-639.

L'Heureux, M. L. A. Butler, B. Jha, A. Kumar, and W. Wang, 2010: Unusual extremes in the negative phase of the Arctic Oscillation during 2009. *Geophys. Res. Lett.*, **37**, L10704, doi: 10.1029/2010GL043338.

Song, Y., and W. A. Robinson, 2004: Dynamical mechanisms for stratospheric influences on the troposphere. *J. Atmos. Sci.*, **61**, 1711-1725.

Thompson, D. W. J., and J. M. Wallace, 1998: The Arctic Oscillation signature in the wintertime geopotential height and temperature fields. *Geophys. Res. Lett.*, **25**, 1297-1300.

Thompson, D.W.J., and J.M. Wallace, 2000: Annular modes in the extratropical circulation. Part I: Month-to-month variability. *J. Climate*, **13**, 1000-1016.

Thompson, D.W.J., and J.M. Wallace, 2001: Regional climate impacts of the Northern Hemisphere Annular Mode. *Science*, **293**, 85-89.

Thompson, D. W. J., J. C. Furtado, and T. G. Shepherd, 2006: On the tropospheric response to anomalous stratospheric wave drag and radiative heating. *J. Atmos. Sci.*, **63**, 2616 – 2629.